AGU PUBLICATIONS

Geophysical Research Letters

RESEARCH LETTER
10.1002/2016GL070438

Key Points:
- A microbial ocean model predicts a larger O_2 deficient zone (ODZ) with slower nitrogen (N) loss than its geochemical approximation
- Resource competition drives gradients in ecological stoichiometry and the dominant microbial pathway of N loss across the ODZ
- Declining O_2 raises the efficiency of N loss within the ODZ, implying a higher sensitivity to climate change than previously predicted

Supporting Information:
- Supporting Information S1
- Figure S1
- Figure S2
- Figure S3
- Figure S4
- Figure S5
- Figure S6
- Figure S7

Correspondence to:
J. Penn,
jpenn@uw.edu

Citation:
Penn, J., T. Weber, and C. Deutsch (2016), Microbial functional diversity alters the structure and sensitivity of oxygen deficient zones, *Geophys. Res. Lett.*, *43*, doi:10.1002/2016GL070438.

Received 15 JUL 2016
Accepted 25 AUG 2016
Accepted article online 28 AUG 2016

Microbial functional diversity alters the structure and sensitivity of oxygen deficient zones

Justin Penn[1], Thomas Weber[1], and Curtis Deutsch[1]

[1]School of Oceanography, University of Washington, Seattle, Washington, USA

Abstract Oxygen deficient zones (ODZs) below the ocean surface regulate marine productivity by removing bioavailable nitrogen (N). A complex microbial community mediates N loss, but the interplay of its diverse metabolisms is poorly understood. We present an ecosystem model of the North Pacific ODZ that reproduces observed chemical distributions yet predicts different ODZ structure, rates, and climatic sensitivity compared to traditional geochemical models. An emergent lower O_2 limit for aerobic nitrification lies below the upper O_2 threshold for anaerobic denitrification, creating a zone of microbial coexistence that causes a larger ODZ but slower total rates of N loss. The O_2-dependent competition for the intermediate nitrite produces gradients in its oxidation versus reduction, anammox versus heterotrophic denitrification, and the net ecological stoichiometry of N loss. The latter effect implies that an externally driven ODZ expansion should favor communities that more efficiently remove N, increasing the sensitivity of the N cycle to climate change.

1. Introduction

The flux of organic matter sinking from the surface ocean can exceed the oxidative capacity of available dissolved O_2 in deeper water. Under the resulting O_2 deficient conditions, the most energetically favorable oxidant is nitrate (NO_3^-), an essential macronutrient for phytoplankton [*Capone et al.*, 2008]. The influence of N removal from the oxygen deficient zones (ODZs) is spread well beyond their small volumes (0.1% of the ocean) to encompass most of the low-latitude surface ocean, where biological productivity is N limited. Geochemical models of the N cycle, which convert NO_3^- directly to N_2 gas with a constant stoichiometry [*Paulmier et al.*, 2009], predict that the rate of total N loss is controlled by the extent of the ODZs and the amount of organic matter they receive [*Moore and Doney*, 2007; *Bianchi et al.*, 2012; *Deutsch et al.*, 2011, 2014].

The loss of N results from a diverse microbial community exchanging multiple N-bearing substrates through interdependent metabolic pathways [*Lam and Kuypers*, 2011]. The first step of heterotrophic denitrification yields NH_4^+ from organic matter and NO_2^- from the initial reduction of NO_3^-. These products can fuel autotrophic bacteria, including anaerobic ammonia oxidizers (anammox bacteria) [*Dalsgaard et al.*, 2003] and two groups of aerobic nitrifiers (NH_4^+ and NO_2^- oxidizers). Anammox bacteria combine the metabolites to form N_2, while the nitrifiers reoxidize them to NO_3^-, diverting NO_2^- from further reduction by heterotrophs [*Anderson et al.*, 1982]. Competition for the scarce intermediates can therefore either enhance or short-circuit the N loss process. The rates of these three metabolic pathways in the major ODZs are highly variable and unpredictable, and their relative importance to long-term N cycling remains controversial [*Kuypers et al.*, 2005; *Ward et al.*, 2009; *Beman et al.*, 2013; *Dalsgaard et al.*, 2012; *Ward*, 2013; *Peng et al.*, 2015].

2. Methods

To investigate the effect of diverse metabolisms on the large-scale rates and stoichiometry of N loss we developed a microbial ecosystem model that simulates the biogeochemical cycles of N and O_2 (Figure S1a in the supporting information). Organic matter is formed by phytoplankton in the surface ocean and is remineralized by four microbial populations. Heterotrophic bacteria are facultative denitrifiers, switching from oxic respiration to a multistep denitrification (reduction of NO_3^- to NO_2^-, then to N_2) when O_2 falls below a critical threshold (O_2^{crit}) [*Devol*, 1978; *Zamora et al.*, 2012; *Brewer et al.*, 2014]. The NH_4^+ released from organic N is used by three autotrophic species: anammox bacteria with a slow and O_2-inhibited growth rate [*Jensen et al.*, 2008; *Kalvelage et al.*, 2011; *Kartal et al.*, 2012; *Dalsgaard et al.*, 2014] and aerobic NH_4^+ oxidizing archaea and NO_2^- oxidizing bacteria with nanomolar O_2 sensitivities [*Kalvelage et al.*, 2011, 2013; *Tiano et al.*, 2014].

Autotrophs assimilate NH_4^+ for cellular structure, while heterotrophs utilize dissolved organic nitrogen (DON), which is released by phytoplankton, sinking particles, and all populations upon mortality. Microbial parameters including growth and mortality rates, nutrient kinetics, and O_2 sensitivities were taken from appropriate laboratory measurements where available (Table S1 in the supporting information).

Microbial biomass and chemical tracers were simulated in an ocean model covering the world's largest ODZ, in the eastern tropical North Pacific (ETNP) [*Karstensen et al*., 2008]. We used an ocean general circulation model that is optimized to fit tracer observations (temperature, salinity, ^{14}C, and CFCs), with a horizontal resolution of 2° latitude and longitude and 24 vertical levels [*DeVries and Primeau*, 2011, ; *DeVries et al*., 2012]. Tracer transport was computed using an annual-mean flow field within the ETNP domain, which extends from the equator to 35°N, the coast to 180°W, and the surface ocean to 2000 m depth. Observed annual mean concentrations of O_2 and NO_3^- from the 2009 World Ocean Atlas [*Antonov et al*., 2010] were transported into the domain at its open boundaries. This ensures that the fidelity of solutions reflects model skill for ODZ processes alone and prevents remote and unrelated errors from propagating into the region of interest.

To determine the sensitivity of model predictions to uncertainty in microbial traits, we conducted model simulations across a wide swath of parameter space. Microbial growth and mortality rates and nutrient half-saturations were varied by an order of magnitude, and the O_2 tolerances of heterotrophs and anammox bacteria were shifted from 1 to 10 and 15 μM, respectively [*Babbin et al*., 2014; *Brewer et al*., 2014; *Devol*, 1978; *Dalsgaard et al*., 2014; *Zamora et al*., 2012; *Kalvelage et al*., 2011, 2015]. Each of the 89 resulting model solutions was vetted using field data from the ETNP, including climatological distributions of NO_3^- and O_2 and profile compilations of NH_4^+, NO_2^-, and excess N_2 gas (Figure 1). Parameter combinations that could not reproduce all tracer distributions simultaneously were not used for further analysis (Figure S2 and Table S1). A representative parameter set was chosen as our standard model case and integrated for 250 years to achieve a long-term steady state. A more detailed description of the methodology can be found in the supporting information [*Betlach and Tiedje*, 1981; *Parsonage et al*., 1985; *Servais et al*., 1985; *Fasham et al*., 1990; *Anderson*, 1995; *Fukuda et al*., 1998; *Strous et al*., 1998; *Koch et al*., 2000; *Rittmann and McCarty*, 2001; *Dalsgaard and Thamdrup*, 2002; *Van Mooy et al*., 2002; *Martens-Habbena et al*., 2009; *Munz et al*., 2011; *Ni et al*., 2011].

3. Results

The model accurately reproduces observed patterns in metabolic rates and the distributions of chemical tracers (Figure 1). The predicted microbial community structure and associated metabolic rates vary between different habitats of the ODZ that are defined by distinct O_2 thresholds (Figures 1a and 1b). Heterotrophic respiration occurs aerobically in oxic water ($O_2 > O_2^{crit}$) [*Devol*, 1978; *Kalvelage et al*., 2015]. In these regions, aerobic-nitrifying populations are the dominant sink for NH_4^- and NO_2^-. These obligate aerobes account for ~17% of O_2 consumption in oxic waters, but are the major consumers of O_2 in the ODZ. Indeed, they determine the lowest O_2 concentration attainable, which occurs when aerobic growth falls below mortality, halting the further consumption of O_2. This break-even O_2 concentration (O_2^*) [*Tilman*, 1982] depends on the nitrifier's half-saturation constants, growth, and mortality rates and defines the core anoxic zone. For the ecosystem model parameters used here, O_2^* ranges from 0.14 to 1.5 nM, consistent with the lowest observed O_2 concentration in the ocean [*Revsbech et al*., 2009; *Thamdrup et al*., 2012; *Tiano et al*., 2014]. In waters with $O_2 = O_2^*$, heterotrophs denitrify NO_3^- to N_2, and anammox bacteria act as the dominant sink for NH_4^+, declining into oxic water because of O_2 inhibition.

Between the two O_2 thresholds, O_2^{crit} and O_2^*, nitrifying and denitrifying populations coexist in a shell of suboxic water that surrounds the anoxic core of the ODZ. The simulated coexistence of these groups is consistent with simultaneous rate measurements [*Lipschultz et al*., 1990; *Füssel et al*., 2011; *Kalvelage et al*., 2013; *Babbin et al*., 2014; *Peng et al*., 2015], paired rate-gene data [*Beman et al*., 2013], and N isotopes [*Casciotti and McIlvin*, 2007; *Buchwald et al*., 2015]. To achieve such coexistence in a steady state requires the O_2 threshold for denitrification (O_2^{crit}) to be above the minimum value required by nitrification (O_2^*). Because the value of O_2^* is constrained by observations to be in the nanomolar range, the overlap between aerobic and anaerobic habitat depends primarily on O_2^{crit}. The model's sensitivity to this uncertain threshold is examined below.

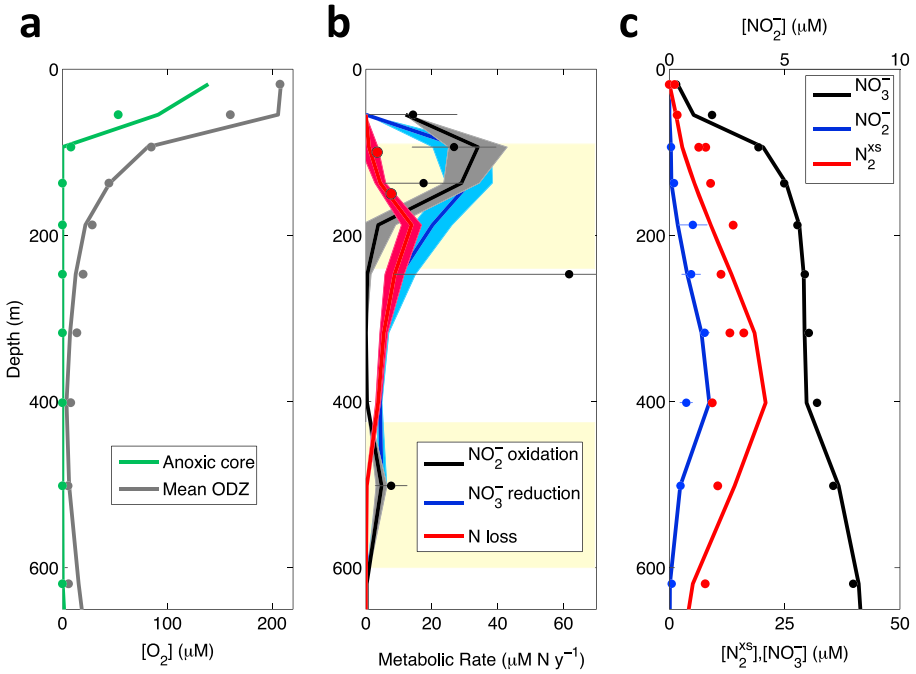

Figure 1. Chemical distributions and metabolic rates from the eastern tropical North Pacific ODZ. Observations (points) are shown with the mean model simulated value (lines) and the standard deviation (shading) among 43 model simulations with different microbial parameters that reproduce all chemical data (see supporting information). (a) Depth profiles of O_2 concentrations taken through the core of the ODZ and averaged over its horizontal extent (Figure S2). The ODZ core profile is computed as the minimum O_2 concentration on a given depth surface. Uncertainty in modeled chemical tracer distributions is smaller than the line thickness. The green points are the measurements from the anoxic core made using a high-precision STOX sensor at station BB2 [*Tiano et al.*, 2014]. The grey points are from the World Ocean Atlas (WOA) annual climatology [*Antonov et al.*, 2010]. (b) Depth profiles of metabolic rates from the core of the ODZ. The coexistence of aerobic and anaerobic processes is marked by yellow bands. NO_2^- oxidation measurements from station 3 of *Beman et al.* [2013] and the offshore stations of *Peng et al.* [2015] are averaged onto the model grid, and their standard error is displayed as horizontal black lines. A single rate outlier lies outside the range displayed (~124 μM N yr^{-1} at 190 m). Observed N loss rates are from offshore in situ particle incubation experiments [*Babbin et al.*, 2014]. Metabolic rates were not used for model vetting and thus provide an independent check on the ecosystem model parameters. (c) Depth profiles of nitrogen compounds averaged over the regions shown in Figure S2. Uncertainty in modeled chemical tracer distributions is smaller than the line thickness. The standard error of NO_2^- observations is shown as horizontal blue lines. Simulated NH_4^+ concentrations (not shown) are at or near the observable detection limit (~10 nM), in agreement with the measurements presented in Figure S2. The NO_2^- data are from *Zamora et al.* [2012], NO_3^- data are from the WOA annual climatology [*Antonov et al.*, 2010], and excess N_2 gas measurements are from *Chang et al.* [2012].

The microbial metabolic rates are also recorded in the observed distributions of key metabolites, providing strong constraints on time-mean community structure. Within the anoxic zone, the net reduction of NO_3^- to NO_2^- forestalls the downward increase in NO_3^-, shunting it into a subsurface maximum in NO_2^- (Figure 1c) [*Ward et al.*, 2009; *Thamdrup et al.*, 2012; *Zamora et al.*, 2012]. The further reduction of NO_2^- to N_2 by both heterotrophic and anammox bacteria yields an accumulation of excess N_2 [*Chang et al.*, 2012] with no detectable NH_4^+ in anoxic water [*Babbin et al.*, 2014; *Tiano et al.*, 2014]. In the oxic ocean, aerobic nitrification maintains both NH_4^+ and NO_2^- at low levels without production of N_2. Across a range of parameter sets ($n = 43$; see Table S1), the model simultaneously reproduces these chemical patterns, implying realistic balances among biological nutrient exchanges and physical fluxes. We use this group of model solutions to quantify the effect of both individual physiological traits and the entire microbial ecosystem on the large-scale cycling of O_2 and N.

Of all the microbial traits, the O_2 threshold of denitrification (O_2^{crit}) exerts the strongest influence on the size of the ODZ and its mean volumetric rate of N loss (see supporting information), two key features of ODZ biogeochemistry. As O_2^{crit} is increased from 1 to 10 μM, the volume of the ODZ defined by that threshold grows by nearly threefold (Figure 2a), in simulations as in climatological observations [*Deutsch et al.*, 2011]. In contrast, the mean rate of N loss declines by a fraction similar to the increase in ODZ size (Figure 2b). The net

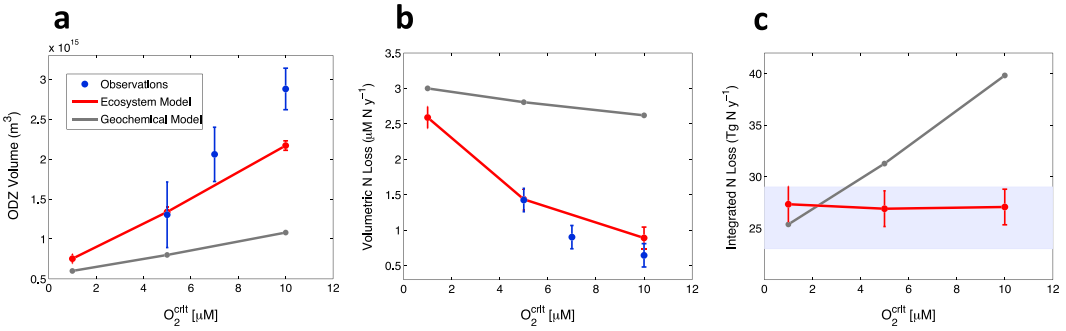

Figure 2. (a) Annual mean ODZ volume and (b) the volumetric and (c) integrated rates of N loss from observations and predicted by the microbial ecosystem and geochemical models, as a function of the critical O_2 threshold for denitrification (O_2^{crit}). ODZ volume is computed as the volume of water with $O_2 < O_2^{crit}$ in the upper 700 m, where the rate of N loss is significant. The error bars on observed volumes represent their monthly standard deviations. Observed volumetric rates are computed by dividing the total rate of N loss [*DeVries et al.*, 2012] by the observed annual ODZ volumes in Figure 2a. The error in the observed volumetric rates represents the 1σ uncertainty in the total rate of N loss, which is shown as greyish blue shading in Figure 2c. Ecosystem model error bars are computed as the standard deviation among data-fitting simulations for the scenario in which $O_2^{crit} = 5$ μM (Figure S3).

effect of this trade-off between volume and volumetric rate is that the ecosystem model maintains a constant total rate of N_2 production (Figure 2c) as well as of regional O_2 consumption (not shown), irrespective of the O_2 concentration at which denitrification begins. Although increases in O_2^{crit} reduce aerobic heterotrophic respiration, that change is compensated for by increases in O_2 consumption via NO_2^- oxidation coupled to heterotrophic NO_3^- reduction in the suboxic zone. These pathways have the same O_2 demand and net NO_3^- yield per unit DON remineralization [*Lam and Kuypers*, 2011]. The O_2 threshold for denitrification therefore cannot be reliably inferred from distributions of O_2, NO_3^-, or N_2.

The insensitivity of integrated N loss to O_2^{crit} in the ecosystem model differs markedly from the predictions of traditional geochemical models, which do not explicitly represent microbial populations. Geochemical models assume no resource competition between nitrifying and denitrifying microbes and can be mimicked in the ecosystem model by excluding nitrifying populations from the ODZ (Figure S1b). Across the simulated range in O_2^{crit}, the ecosystem model produces an ODZ that is 25% to 100% larger than the geochemical approximation (Figure 2a) but with rates of N loss that are 14% to 66% slower on average (Figure 2b). These differences are independent of microbial growth and mortality rates and nutrient half-saturations (Figure S3). In contrast to the ecosystem model, regional N loss from the geochemical model increases with O_2^{crit} because it causes the ODZ volume to rise without a concomitant reduction in volumetric N loss. As O_2^{crit} decreases, so does the overlap of aerobic and anaerobic habitat, causing the ecosystem and geochemical models to converge.

The ecosystem's dilution of N loss across a more expansive ODZ results from interactions between nitrifying and denitrifying bacteria. Nitrifiers are assumed to have a lower half-saturation constant for NO_2^- than the heterotrophic populations (Table S1), giving them a competitive advantage when O_2 is available. Indeed, this higher NO_2^- affinity is required in the model to reproduce the observed lack of NO_2^- in oxic water and its accumulation in anoxic waters (Figure 1). As a result of this advantage, nitrifying bacteria that thrive in the suboxic shell surrounding the core anoxic zone limit complete heterotrophic denitrification to N_2 by reoxidizing NO_2^- produced by the first step of denitrification (Figure 3a). The additional consumption of O_2 by nitrifiers leads to the simulated growth of the ODZ relative to the geochemical model, in which NO_2^- reoxidation is precluded. While concentrated at the boundaries of the anoxic zone, where O_2 falls below the detection limit of traditional methods, NO_2^- oxidation continues into the core [*Peng et al.*, 2015], maintaining O_2 at levels below the detection limit of the most sensitive sensors [*Revsbech et al.*, 2009; *Tiano et al.*, 2014]. In the anoxic core, O_2 limitation of NO_2^- oxidation allows NO_2^- to accumulate, favoring complete heterotrophic denitrification to N_2.

The competitive advantage of NO_2^- oxidizers in the suboxic shell reduces the mean volumetric rate of N_2 production via its effect on the average stoichiometry of N loss (Figure 3b). By diverting NO_2^- from further reduction, nitrifying bacteria substantially lower the total amount of N_2 produced per mole of DON

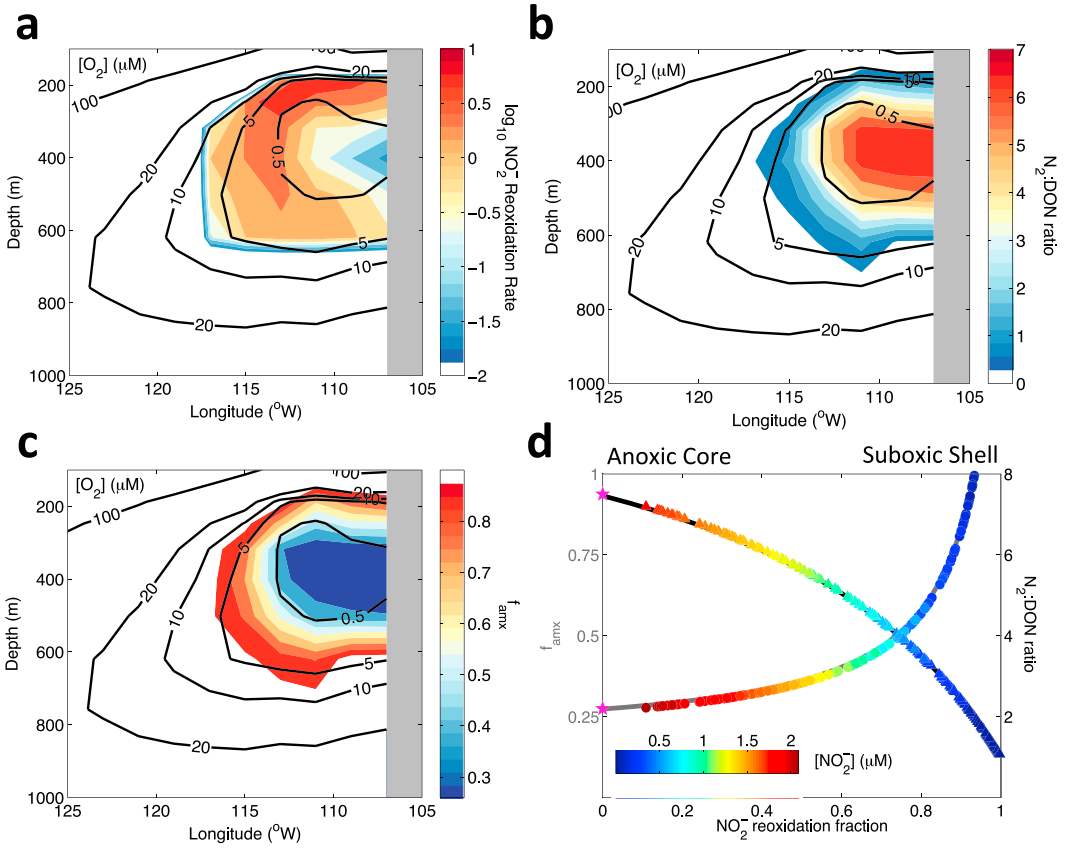

Figure 3. Cross sections through the ODZ of (a) the NO_2^- reoxidation rate (μM N yr^{-1}), (b) the ratio of total N_2 produced per mole of DON remineralized via denitrification (N_2:DON ratio), and (c) the contribution of anammox to total N loss (f_{amx}) from the standard ecosystem model scenario. NO_2^- reoxidation is defined as NO_2^- that is produced from NO_3^- during the first step of heterotrophic denitrification but is oxidized back to NO_3^- during nitrification. Note the $\log_{10}$ scaling of NO_2^- reoxidation rates in Figure 3a. Rates and ratios are overlain by time-mean O_2 concentrations (contours). The grey shading denotes the eastern boundary of the Pacific Ocean. (d) N_2:DON ratios (triangles) and f_{amx} (circles) versus the NO_2^- reoxidation fraction from the standard ecosystem model scenario. The NO_2^- reoxidation fraction includes the accumulation of NO_2^- (colors) in the anoxic core, which is eventually reoxidized to NO_3^- in the suboxic shell. Model values conform exactly to steady state predictions (lines; grey for f_{amx} and black for N_2:DON) based on the known reaction stoichiometries (see supporting information) [*Koeve and Kähler*, 2010]. The values predicted by geochemical models are shown as pink stars.

remineralized by heterotrophic denitrifiers (herein the N_2:DON ratio), below the 7.5 assumed in traditional geochemical models (Figure S4) [*Paulmier et al.*, 2009]. Depending on the value of O_2^{crit}, the mean N_2:DON ratio in the suboxic shell lies between 3.9 and 1.4. As O_2^{crit} is increased, this decreases the ODZ's average stoichiometry of N loss by expanding the niche of NO_2^- oxidizers. The O_2^{crit} threshold defines the volume of the suboxic shell, where NO_2^- oxidizers are dominant, but not the anoxic core, where NO_2^- uptake is controlled by denitrification. Increases in O_2^{crit} thus raise the ratio of suboxic to anoxic water, which shifts the stoichiometry of N loss toward the low values found in the suboxic shell, causing the slower mean volumetric rate of N loss (Figure 2b). In the geochemical model, volumetric N loss is maintained even as O_2^{crit} is increased, because it lacks a suboxic zone in which NO_2^- oxidation outcompetes heterotrophic denitrification.

Associated with these stoichiometric gradients are large variations in the fraction of N loss contributed by autotrophic anammox bacteria versus the heterotrophs, denoted f_{amx} (Figure 3c). The attribution of N_2 production to these different populations from direct rate measurements in the field has proven controversial due to substantial variability with unknown cause [*Kuypers et al.*, 2005; *Ward et al.*, 2009; *Dalsgaard et al.*, 2012; *Kalvelage et al.*, 2013; *Ward*, 2013]. The microbial ecosystem produces spatial variations in f_{amx} as a natural consequence of resource competition in the suboxic zone. In contrast to heterotrophs, the uptake of NO_2^- by nitrifiers has little effect on anammox bacteria because they are NH_4^+ limited [*Dalsgaard et al.*,

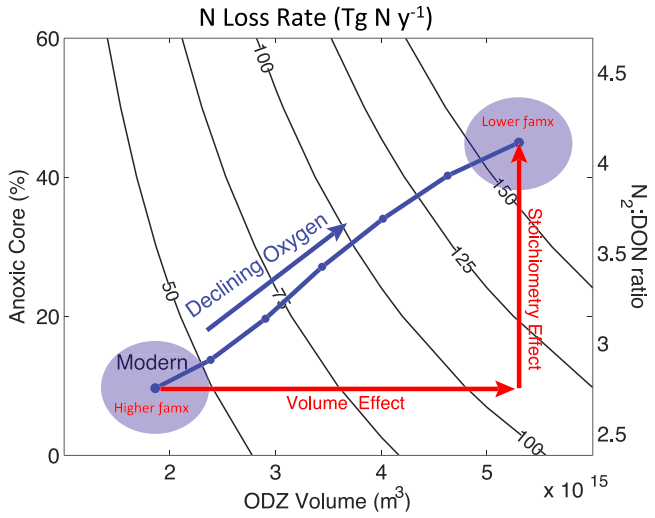

Figure 4. Predicted rates of N loss in the Pacific Ocean (contours; Tg N yr^{-1}) for a given total ODZ volume, anoxic volume percentage, and ratio of total N_2 produced per mole of DON remineralized via denitrification (N_2:DON ratio). N loss rates are computed as $J^{N2} = J^{DON}(r^{anx}V^{anx} + r^{sub}V^{sub})$, where r^{anx} is the N_2:DON ratio in the anoxic core (6.2), r^{sub} is the N_2:DON ratio in the suboxic shell (2.4), J^{DON} is the mean anaerobic remineralization rate (7.6×10^{-15} Tg N m^{-3} yr^{-1}), and V^{anx} and V^{sub} are the potential volumes (m^3) of anoxic and suboxic waters, respectively. N_2:DON ratios and rates of anaerobic DON remineralization are diagnosed from the standard ecosystem model scenario. The solid blue line is the relationship between annual mean ODZ volume and its anoxic percentage in the Pacific Ocean, as derived from the World Ocean Atlas climatology [*Antonov et al.*, 2010], assuming the ODZ starts at $O_2 < 5$ μM. Uncertainty in modern ocean values (blue shading around the leftmost point) is calculated as the standard deviation across monthly observations and is propagated to the deoxygenated ODZ. Potential volumes and anoxic percentages (points to the right of modern) are calculated from observations by subtracting O_2 in increasing 1 μM increments in a spatially uniform pattern. The component of N loss change that results from a change in mean N loss stoichiometry is indicated by the vertical red vector, while the component that results from a total volume change is indicated by the horizontal vector.

2003; *Lam and Kuypers*, 2011]. The fractional contribution of anammox to N_2 production is therefore greatest in the suboxic shell, and declines into the anoxic core of the ODZ, where reoxidation is slowed by scarce O_2. Integrated across the ODZ, anammox contributes to between 31% and 49% of N loss (i.e., $f_{amx} = 0.31$–0.49; see section S5 and Figure S5 in the supporting information).

The stoichiometry of steady state anaerobic reactions is thought to imply a mean f_{amx} of 0.28 [*Koeve and Kähler*, 2010] but cannot explain the large observed deviations from this value. Previous studies assume that all NO_2^- produced by denitrification is reduced to N_2 [*Babbin et al.*, 2014]. When accounting for the fraction of NO_2^- that is oxidized or accumulates in the water column, simulated spatial variabilities of both f_{amx} and N_2:DON can be predicted exactly (Figure 3d). The niche partitioning of aerobic and anaerobic metabolisms along gradients in O_2 can thus reconcile variations in f_{amx} and simple mass balance predictions, without the need for non-Redfieldian organic matter cycling [*Babbin et al.*, 2014] or supplementary sources of NH_4^+ [*Lam et al.*, 2009; *Bianchi et al.*, 2014].

4. Sensitivity of N Loss to Deoxygenation

The gradient of N loss stoichiometry associated with the mean microbial habitat pattern implies a greater sensitivity of the N cycle to climate than previously recognized (Figure 4). The volume of low O_2 water undergoing N loss is itself quite sensitive to climate-driven changes in tropical O_2 [*Deutsch et al.*, 2011], but changes in N loss also depend on the ratio of total N_2 production per unit of organic N remineralization via denitrification, which have not been previously considered. Because N_2:DON ratios increase systematically from the suboxic shell to the anoxic core (Figure 3b), any increase in the ratio of anoxic to suboxic water volume should also accelerate N loss and shift the balance of metabolisms in favor of heterotrophic denitrification over anammox.

To demonstrate this stoichiometric effect, we simulated the influence of a large-scale O_2 depletion on the contemporary volumes of anoxic and suboxic waters in the Pacific Ocean, by applying a uniform anomaly to the current climatological O_2 distribution. These idealized O_2 depletion experiments approximate the response of the ODZ's volume to historical climate variations in more realistic models [*Deutsch et al.*, 2011]. As O_2 is depleted on the regional scale, the volume of anoxic and suboxic waters both rise, as expected (Figure 4). However, the anoxic water expands proportionally faster, increasing the ratio of the anoxic core volume relative to that of the suboxic shell. Although observational uncertainties in current climatological volumes are considerable, an increase in the core to shell volume ratio is robust to these uncertainties (Figure S6) because it arises from simple geometry; a bounded volume grows proportionally faster than its surrounding surface.

To estimate the consequence of these volume changes for total N loss rates, we applied the model-predicted gradients in ecosystem stoichiometry throughout the Pacific ODZ. By altering mean N loss stoichiometry, shifts in the relative volumes of these distinct microbial habitat zones further increase N loss by an amount comparable to the ODZ volume expansion itself (Figure 4), thus doubling the impact of O_2 depletion in the metabolically diverse ocean compared to one with fixed N-cycle stoichiometry. A full accounting of the long-term effect of ocean deoxygenation and climate warming on N loss must take into account interactions between ocean circulation, N loss, and biological export, which our calculations have held constant. However, these idealized calculations illustrate a novel and important role for changing ecological stoichiometry due to shifts in the microbial community across the ODZ as the ocean loses O_2. Accurately predicting the response of N loss to climate change will therefore require ocean models to account for feedback between these microbial ecosystem dynamics and the biogeochemical cycles.

Acknowledgments

We thank B. Chang for the NH_4^+ data, T. DeVries for the ocean circulation model, C. Fuchsman for the NO_2^- oxidation and STOX O_2 data, and A. Santoro for the valuable feedback. The data used in this work are listed in the references, tables, and supplements and are available upon request. This work was supported by a grant from the Gordon and Betty Moore Foundation (GBMF #3775).

References

Anderson, J. J., A. Okubo, A. S. Robbins, and F. A. Richards (1982), A model for nitrate distributions in oceanic oxygen minimum zones, *Deep Sea Rese. Oceanogr. Res. Paper.*, *29*(9), 1113–1140.

Anderson, L. A. (1995), On the hydrogen and oxygen content of marine phytoplankton, *Deep Sea Res., Part I*, *42*(9), 1675–1680.

Antonov, J. I., D. Seidov, T. P. Boyer, R. A. Locarnini, A. V. Mishonov, H. E. Garcia, O. K. Baranova, M. M. Zweng, and D. R. Johnson (2010), World ocean database 2009. In NOAA Atlas NESDIS 66 (US Govt Printing Office).

Babbin, A. R., R. G. Keil, A. H. Devol, and B. B. Ward (2014), Organic matter stoichiometry, flux, and oxygen control nitrogen loss in the ocean, *Science*, *344*(6182), 406–408.

Beman, J. M., J. L. Shih, and B. N. Popp (2013), Nitrite oxidation in the upper water column and oxygen minimum zone of the eastern tropical North Pacific Ocean, *ISME J.*, *7*(11), 2192–2205.

Betlach, M. R., and J. M. Tiedje (1981), Kinetic explanation for accumulation of nitrite, nitric oxide, and nitrous oxide during bacterial denitrification, *Appl. Environ. Microbiol.*, *42*(6), 1074–1084.

Bianchi, D., J. P. Dunne, J. L. Sarmiento, and E. D. Galbraith (2012), Data-based estimates of suboxia, denitrification, and N_2O production in the ocean and their sensitivities to dissolved O_2, *Global Biogeochem. Cycles*, *26*, GB2009, doi:10.1029/2011GB004209.

Bianchi, D., A. R. Babbin, and E. D. Galbraith (2014), Enhancement of anammox by the excretion of diel vertical migrators, *Proc. Natl. Acad. Sci. U.S.A.*, *111*(44), 15,653–15,658.

Brewer, P. G., A. F. Hofmann, E. T. Peltzer, and W. Ussler (2014), Evaluating microbial chemical choices: The ocean chemistry basis for the competition between use of O_2 or NO_3- as an electron acceptor, *Deep Sea Res., Part I*, *87*, 35–42.

Buchwald, C., A. E. Santoro, R. H. R. Stanley, and K. L. Casciotti (2015), Nitrogen cycling in the secondary nitrite maximum of the eastern tropical North Pacific off Costa Rica, *Global Biogeochem. Cycles*, *29*, 2061–2081, doi:10.1002/2015GB005187.

Capone, D. G., D. A. Bronk, M. R. Mulholland, and E. J. Carpenter (2008), *Nitrogen in the Marine Environment*, Academic Press, Burlington, Mass.

Casciotti, K., and M. McIlvin (2007), Isotopic analyses of nitrate and nitrite from reference mixtures and application to eastern tropical North Pacific waters, *Mar. Chem.*, *107*(2), 184–201.

Chang, B. X., A. H. Devol, and S. R. Emerson (2012), Fixed nitrogen loss from the eastern tropical North Pacific and Arabian Sea oxygen deficient zones determined from measurements of N_2:Ar, *Global Biogeochem. Cycles*, *26*, GB3030, doi:10.1029/2011GB004207.

Dalsgaard, T., and B. Thamdrup (2002), Factors controlling anaerobic ammonium oxidation with nitrite in marine sediments, *Appl. Environ. Microbiol.*, *68*, 3802–3808.

Dalsgaard, T., D. E. Canfield, J. Petersen, B. Thamdrup, and J. Acuña-González (2003), N_2 production by the anammox reaction in the anoxic water column of Golfo Dulce, Costa Rica, *Nature*, *422*(6932), 606–608.

Dalsgaard, T., B. Thamdrup, L. Farías, and P. N. Revsbech (2012), Anammox and dentrification in the oxygen minimum zone of the eastern South Pacific, *Limnol. Oceanogr.*, *57*(5), 1331.

Dalsgaard, T., F. J. Stewart, B. Thamdrup, L. De Brabandere, N. P. Revsbech, O. Ulloa, D. E. Canfield, and E. F. Delong (2014), Oxygen at nanomolar levels reversibly suppresses process rates and gene expression in anammox and denitrification in the oxygen minimum zone off northern Chile, *mBio*, *5*, e01966.

Deutsch, C., H. Brix, T. Ito, H. Frenzel, and L. Thompson (2011), Climate forcing of ocean hypoxia, *Science*, *333*, 336–339.

Deutsch, C., et al. (2014), Centennial changes in North Pacific anoxia linked to tropical trade winds, *Science*, *345*(6197), 665–668.

Devol, A. H. (1978), Bacterial oxygen uptake kinetics as related to biological processes in oxygen deficient zones of the oceans, *Deep Sea Res.*, *25*(2), 137–146.

DeVries, T., and F. Primeau (2011), Dynamically and observationally constrained estimates of water-mass distributions and ages in the global ocean, *J. Phys. Oceanogr.*, *41*, 2381–2401.

DeVries, T., C. Deutsch, F. Primeau, B. Chang, and A. Devol (2012), Global rates of water-column denitrification derived from nitrogen gas measurements, *Nat. Geosci.*, *5*, 1–4.

Fasham, M., H. Ducklow, and S. McKelvie (1990), A nitrogen-based model of plankton dynamics in the oceanic mixed layer, *J. Mar. Res.*, *48*, 591–639.

Fukuda, R., H. Ogawa, and T. Nagata (1998), Direct determination of carbon and nitrogen contents of natural bacterial assemblages in marine environments, *Appl. Environ. Microbiol.*, *64*, 3352–3358.

Füssel, J., P. Lam, G. Lavik, M. M. Jensen, M. Holtappels, M. Günter, and M. M. Kuypers (2011), Nitrite oxidation in the Namibian oxygen minimum zone, *ISME J.*, *6*(6), 1200–1209.

Jensen, M. M., M. M. Kuypers, G. Lavik, and B. Thamdrup (2008), Rates and regulation of anaerobic ammonium oxidation and denitrification in the Black Sea, *Limnol. Oceanogr.*, *53*(1), 23.

Kalvelage, T., M. M. Jensen, S. Contreras, N. Peter Revsbech, P. Lam, M. Günter, J. LaRoche, G. Lavik, and M. M. M. Kuypers (2011) Oxygen sensitivity of anammox and coupled N-cycle processes in oxygen minimum zones. *PLoS One*, *6*(12), e29299, doi:10.1371/journal.pone.0029299.

Kalvelage, T., G. Lavik, P. Lam, S. Contreras, L. Arteaga, C. R. Löscher, A. Oschlies, A. Paulmier, L. Stramma, and M. M. M. Kuypers (2013), Nitrogen cycling driven by organic matter export in the South Pacific oxygen minimum zone, *Nat. Geosci.*, *6*(3), 228–234.

Kalvelage, T., et al. (2015) Aerobic microbial respiration in oceanic oxygen minimum zones, *PLoS One*, *10*(7), e0133526, doi:10.1371/journal.pone.0133526

Karstensen, J., L. Stramma, and M. Visbeck (2008), Oxygen minimum zones in the eastern tropical Atlantic and Pacific Oceans, *Prog. Oceanogr.*, *77*, 331–350.

Kartal, B., L. van Niftrik, J. T. Keltjens, H. J. Op den Camp, and M. S. Jetten (2012), Anammox—Growth physiology, cell biology, and metabolism, *Adv Microb. PhysiOl.*, *60*, 212.

Koch, G., K. Egli, J. Van der Meer, and H. Siegrist (2000), Mathematical modeling of autotrophic denitrification in a nitrifying biofilm of a rotating biological contactor, *Water Sci. Technol.*, *41*, 191–198.

Koeve, W., and P. Kähler (2010), Heterotrophic denitrification vs. autotrophic anammox—Quantifying collateral effects on the oceanic carbon cycle, *Biogeosciences*, *7*(8), 2327–2337.

Kuypers, M. M. M., G. Lavik, D. Woebken, M. Schmid, B. M. Fuchs, R. Amann, B. B. Jørgensen, and M. S. M. Jetten (2005), Massive nitrogen loss from the Benguela upwelling system through anaerobic ammonium oxidation, *Proc. Natl. Acad. Sci. U.S.A.*, *102*(18), 6478–6483.

Lam, P., and M. M. Kuypers (2011), Microbial nitrogen cycling processes in oxygen minimum zones, *Annu. Rev. Mar. Sci.*, *3*, 317–345.

Lam, P., G. Lavik, M. M. Jensen, J. van de Vossenberg, M. Schmid, D. Woebken, D. Gutiérrez, R. Amann, M. S. M. Jetten, and M. M. M. Kuypers (2009), Revising the nitrogen cycle in the Peruvian oxygen minimum zone, *Proc. Natl. Acad. Sci. U.S.A.*, *106*(12), 4752–4757.

Lipschultz, F., C. Wofsy, B. B. Ward, L. A. Codispoti, G. J. W. Friedrich, and J. W. Elkins (1990), Bacterial transformations of inorganic nitrogen in the oxygen-deficient waters of the eastern tropical South Pacific Ocean, *Deep Sea Res. Oceanogr. Res. Paper.*, *37*(10), 1513–1541.

Martens-Habbena, W., P. M. Berube, H. Urakawa, J. R. de La Torre, and D. A. Stahl (2009), Ammonia oxidation kinetics determine niche separation of nitrifying archaea and bacteria, *Nature*, *461*, 976–979.

Moore, J. K., and S. C. Doney (2007), Iron availability limits the ocean nitrogen inventory stabilizing feedbacks between marine denitrification and nitrogen fixation, *Global Biogeochem. Cycles*, *21*, GB2001, doi:10.1029/2006GB002762.

Munz, G., C. Lubello, and J. A. Oleszkiewicz (2011), Factors affecting the growth rates of ammonium and nitrite oxidizing bacteria, *Chemosphere*, *83*, 720–725.

Ni, B. J., M. Ruscalleda, C. Pellicer-Nacher, and B. F. Smets (2011), Modeling nitrous oxide production during biological nitrogen removal via nitrification and denitrification: Extensions to the general ASM models, *Environ. Sci. Technol.*, *45*(18), 7768–7776.

Parsonage, D., A. J. Greenfield, and S. J. Ferguson (1985), The high affinity of *Paracoccus denitrificans* cells for nitrate as an electron acceptor. Analysis of possible mechanisms of nitrate and nitrite movement across the plasma membrane and the basis for inhibition by added nitrite of oxidase activity in permeabilised cells, *Biochim. Biophys. Acta (BBA)-Bioenergetics*, *807*, 81–95.

Paulmier, A., I. Kriest, and A. Oschlies (2009), Stoichiometries of remineralisation and denitrification in global biogeochemical ocean models, *Biogeosciences (BG)*, *6*, 923–935.

Peng, X., C. A. Fuchsman, A. Jayakumar, S. Oleynik, W. Martens-Habbena, A. H. Devol, and B. B. Ward (2015), Ammonia and nitrite oxidation in the eastern tropical North Pacific, *Global Biogeochem. Cycles*, *29*, 2034–2049, doi:10.1002/2015GB005278.

Revsbech, N. P., L. H. Larsen, J. Gundersen, T. Dalsgaard, O. Ulloa, and B. Thamdrup (2009), Determination of ultra-low oxygen concentrations in oxygen minimum zones by the STOX sensor, *Limnol. Oceanogr. Methods*, *7*, 371–381.

Rittmann, B. E., and P. L. McCarty (2001), *Environmental Biotechnology: Principles and Applications*, Tata McGraw-Hill Education, New York.

Servais, P., G. Billen, and J. V. Rego (1985), Rate of bacterial mortality in aquatic environments, *Appl. Environ. Microbiol.*, *49*, 1448–1454.

Strous, M., J. Heijnen, J. Kuenen, and M. Jetten (1998), The sequencing batch reactor as a powerful tool for the study of slowly growing anaerobic ammonium-oxidizing microorganisms, *Appl. Microbiol. Biotechnol.*, *50*(5), 589–596.

Thamdrup, B., T. Dalsgaard, and N. P. Revsbech (2012), Widespread functional anoxia in the oxygen minimum zone of the eastern South Pacific, *Deep Sea Res., Part I*, *65*, 36–45.

Tiano, L., E. Garcia-Robledo, T. Dalsgaard, A. H. Devol, B. B. Ward, O. Ulloa, D. E. Canfieldf, and N. P. Revsbech (2014), Oxygen distribution and aerobic respiration in the north and south eastern tropical Pacific oxygen minimum zones, *Deep Sea Res., Part I*, *94*, 173–183.

Tilman, D. (1982), *Resource Competition and Community Structure. Monographs in Population Biology*, Princeton University Press, Princeton, N. J.

Van Mooy, B. A. S., R. G. Keil, and A. H. Devol (2002), Impact of suboxia on sinking particulate organic carbon: Enhanced carbon flux and preferential degradation of amino acids via denitrification, *Geochim. Cosmochim. Acta*, *66*(3), 457–465.

Ward, B. B. (2013), How nitrogen is lost, *Science*, *341*, 352.

Ward, B. B., A. H. Devol, J. J. Rich, B. X. Chang, S. E. Bulow, H. Naik, A. Pratihary, and A. Jayakumar (2009), Denitrification as the dominant nitrogen loss process in the Arabian Sea, *Nature*, *461*(7260), 78–U77.

Zamora, L., A. Oschlies, H. W. Bange, K. B. Huebert, J. D. Craig, A. Kock, and C. R. Löscher (2012), Nitrous oxide dynamics in low oxygen regions of the Pacific: Insights from the MEMENTO database, *Biogeosciences (BG)*, *9*, 5007–5022.